

Liprin-Mediated Large Signaling Complex Organization Revealed by the Liprin- α /CASK and Liprin- α /Liprin- β Complex Structures

Zhiyi Wei,^{1,2,5} Suilan Zheng,^{1,5} Samantha A. Spangler,⁴ Cong Yu,^{1,*} Casper C. Hoogenraad,^{3,4} and Mingjie Zhang^{1,*}

¹Division of Life Science, State Key Laboratory of Molecular Neuroscience, Molecular Neuroscience Center

²Institute for Advanced Study

Hong Kong University of Science and Technology, Clear Water Bay, Kowloon, Hong Kong, China

³Cell Biology, Faculty of Science, Utrecht University, 3508 TC Utrecht, The Netherlands

⁴Department of Neuroscience, Erasmus Medical Center, 3015 CE Rotterdam, The Netherlands

⁵These authors contributed equally to this work

*Correspondence: yucong@ust.hk (C.Y.), mzhang@ust.hk (M.Z.)

DOI 10.1016/j.molcel.2011.07.021

SUMMARY

Liprins are highly conserved scaffold proteins that regulate cell adhesion, cell migration, and synapse development by binding to diverse target proteins. The molecular basis governing liprin/target interactions is poorly understood. The liprin- α 2/CASK complex structure solved here reveals that the three SAM domains of liprin- α form an integrated supramodule that binds to the CASK kinase-like domain. As supported by biochemical and cellular studies, the interaction between liprin- α and CASK is unique to vertebrates, implying that the liprin- α /CASK interaction is likely to regulate higher-order brain functions in mammals. Consistently, we demonstrate that three recently identified X-linked mental retardation mutants of CASK are defective in binding to liprin- α . We also solved the liprin- α /liprin- β SAM domain complex structure, which uncovers the mechanism underlying liprin heterodimerization. Finally, formation of the CASK/liprin- α /liprin- β ternary complex suggests that liprins can mediate assembly of target proteins into large protein complexes capable of regulating numerous cellular activities.

INTRODUCTION

Liprins, originally identified as binding partners of the receptor protein tyrosine phosphatase LAR (leukocyte common antigen-related) (Serra-Pagès et al., 1998), are known to play roles in many cellular processes, including cell migration, cell adhesion, lymphatic vessel development, and synaptic development and activity (Astigarraga et al., 2010; Choe et al., 2006; Dai et al., 2006; Dunah et al., 2005; Kaufmann et al., 2002; Olsen et al., 2005; Schoch et al., 2002; Shen et al., 2007; Wyszynski et al., 2002; Zhen and Jin, 1999). Vertebrates contain two families of liprins, liprin- α and liprin- β , which have four (α 1, α 2, α 3, and α 4) and two (β 1 and β 2) members, respectively (Serra-Pagès et al.,

1998). In contrast, *C. elegans* and *Drosophila* each contain only one liprin- α , called Syd-2 and Dliprin- α , respectively (Kaufmann et al., 2002; Zhen and Jin, 1999). All isoforms of liprins share highly similar domain organizations, consisting of an N-terminal coiled-coil domain and a C-terminal liprin homology (LH) region comprised of three sterile alpha motif (SAM) domains (Kaufmann et al., 2002; Serra-Pagès et al., 1998; Zürner and Schoch, 2009) (Figure 1A). The N-terminal coiled coils of liprin- α act as binding regions for several synaptic proteins, including CAST, GIT1, RIM, and KIF1A (Ko et al., 2003a, 2003b; Schoch et al., 2002; Shin et al., 2003). The SAM repeats can bind to both phosphatases (e.g., LAR, PTP δ , and PTP σ) (Serra-Pagès et al., 1998) and protein kinases (e.g., CASK) (Olsen et al., 2005), although the molecular basis of these interactions is unknown. Additionally, the SAM repeats of liprin- α and liprin- β can form heterodimers (Serra-Pagès et al., 1998), although again the underlying molecular mechanism is unknown.

Much of our current understanding of the functions of liprin is derived from extensive studies in neurons. In *C. elegans* and *Drosophila*, loss-of-function mutations of liprin- α result in enlarged active zones, reduced synapse formation, impaired synaptic transmission, and mistargeting of axons (Choe et al., 2006; Hofmeyer et al., 2006; Kaufmann et al., 2002; Prakash et al., 2009; Zhen and Jin, 1999), indicating that liprin- α plays critical roles in synaptic development and activity. The specific interaction between liprin- α and CASK in mammals hints that liprin- α may be directly involved in neurotransmitter release as well as the establishment of cell polarity via the highly conserved Veli (also called MALS or mLin-7)/CASK/Mint-1 (or X11 α) tripartite complex (Biederer and Südhof, 2000; Borg et al., 1999; Feng et al., 2004; Hata et al., 1996; Hsueh et al., 1998; Maximov et al., 1999; Kaeck et al., 1998; Olsen et al., 2005, 2007; Samuels et al., 2007; Schoch et al., 2002). Recently, several human genetic studies have revealed that CASK mutations are closely associated with mental retardations (Froyen et al., 2007; Hayashi et al., 2008; Najm et al., 2008; Piluso et al., 2009; Tarpey et al., 2009), although the molecular basis for this association is unknown. The mutation-induced impairment of the liprin- α /CASK interaction may constitute the molecular mechanism underlying the involvement of CASK in mental retardation.

In contrast to the direct physical and functional interaction between liprin- α and CASK observed in mammals, liprin- α does not seem to interact with the CASK ortholog in invertebrates. The loss of function of *liprin- α /Syd-2* in *C. elegans* manifests itself in the form of defects in active zone assembly with enlarged zone areas (Zhen and Jin, 1999), whereas the *Lin-2* defective mutant displayed a vulvaless phenotype (Kaeche et al., 1998). It has also been demonstrated that, at least in HSN neurons in *C. elegans*, liprin- α /Syd-2 and Lin-2 neither colocalize nor genetically interact with each other (Dai et al., 2006; Patel et al., 2006). Given the highly conserved nature of both proteins throughout evolution, it is conceptually challenging to explain the functional differences for liprin- α and CASK between mammals and lower eukaryotes.

To understand the molecular basis of liprin-mediated protein complex assembly, we characterized the liprin- α /CASK and liprin- α /liprin- β interactions in detail. The crystal structure of the liprin- α SAM domain repeats in complex with the CaM kinase (CaMK) domain of CASK reveals unexpected binding modes for both SAM domains and the CaMK domain. Importantly, the structure of the liprin- α /CASK complex reveals that the liprin- α /CASK interaction is specific to vertebrates. We discovered that several mutants of CASK found in X-linked mental retardation (XLMR) patients have decreased affinities for liprin- α . Finally, the structure of the liprin- α /liprin- β SAM repeat complex provides mechanistic insights into the assembly of the CASK/liprin- α /liprin- β ternary suprascaffold.

RESULTS AND DISCUSSION

Mapping of the Interaction between Liprin- $\alpha 2$ and CASK

We chose liprin- $\alpha 2$ for our study because this isoform has been shown to interact specifically with CASK (Olsen et al., 2005; Samuels et al., 2007). The first SAM domain (SAM1) of liprin- $\alpha 2$ was shown to be necessary and sufficient for binding to CASK, and the CaMK domain and the first L27 domain of CASK were shown to be necessary for CASK to interact with liprin- $\alpha 2$ by yeast two-hybrid assay (Olsen et al., 2005) (see Figure 1A for the domain organizations of the two proteins). We first tried to verify the above findings using purified proteins. We found that the inclusion of an ~ 25 -residue extension at both the N and C termini of the canonical SAM1 domain boundary (residues 866–1001 for the extended SAM1) is necessary to obtain folded SAM1 domain. To our surprise, a mixture of the extended SAM1 and CASK_CaMK (with and without the first L27 domain) was eluted as two separate peaks corresponding to the isolated CASK_CaMK and SAM1, respectively, in an analytical gel filtration column, indicating weak or no binding between these two proteins (data not shown). In contrast, the entire LH region of liprin- $\alpha 2$ (liprin- $\alpha 2$ _LH), composed of its three SAM domains, coeluted with CASK_CaMK in the analytical gel filtration column with an elution volume indicative of a molecular mass of ~ 70 kDa (i.e., a 1:1 liprin- $\alpha 2$ _LH/CASK_CaMK complex) (Figure 1B). Isothermal titration calorimetry (ITC)-based assays showed that liprin- $\alpha 2$ _LH binds to CASK_CaMK with a K_d of ~ 0.6 μ M (Figure 1C). Further extension of liprin- $\alpha 2$ _LH did not enhance its CASK binding (Figure 1D), indicating that liprin- $\alpha 2$ _LH contains the complete CASK binding sequence. Consistent

with our gel filtration chromatography results, the extended SAM1 alone binds to CASK_CaMK with a much weaker affinity ($K_d \sim 9$ μ M) (Figures 1C, middle panel, and 1D). We further showed that the first L27 domain of CASK is not required for liprin- $\alpha 2$ binding, as CASK_CaMK alone displayed an affinity for liprin- $\alpha 2$ equal to that of CASK_CaMK together with the first L27 domain (Figure 1D). Taken together, the above biochemical data demonstrate that the three SAM domains of liprin- $\alpha 2$ and the CaMK domain of CASK constitute the necessary and sufficient elements for the two proteins to form a stable complex. The above finding also raises the intriguing question of how three SAM domains together recognize a protein kinase domain, although an isolated SAM domain has been shown to bind to the kinase domain of MAP kinases (Qiao et al., 2006; Seidel and Graves, 2002).

Overall Structure of the Liprin- $\alpha 2$ /CASK Complex

To elucidate the molecular details of the liprin- $\alpha 2$ /CASK interaction, we determined the crystal structure of the liprin- $\alpha 2$ _LH/CASK_CaMK complex at 2.2 Å resolution (Table 1). Consistent with the data shown in Figure 1B, each asymmetric unit of the crystal contains one complex molecule with a 1:1 stoichiometry (Figure 1E). Except for a 20-residue flexible loop (aa 998–1017) connecting SAM1 and SAM2 of liprin- $\alpha 2$ and a few residues at the termini of the two proteins, the electron densities of the rest of the complex were clearly assigned.

In the complex (Figure 1E), CASK_CaMK adopts a typical protein kinase fold. The three SAM domains of liprin- $\alpha 2$ pack sequentially in a head-to-tail manner, forming a linear assembly. The interaction between CASK_CaMK and liprin- $\alpha 2$ is restricted to the C-lobe of the CaMK domain. The SAM1 and SAM2 domains of liprin- $\alpha 2$ make extensive contact with the bottom of the C-lobe of CaMK, and a unique insertion between SAM1 and SAM2 of liprin- $\alpha 2$ wraps around the backside of the CaMK C-lobe (relative to the CaMK catalytic cleft) (Figure 1E). The liprin- $\alpha 2$ _LH/CASK_CaMK complex structure reveals a previously unknown interaction mode for SAM domains. SAM domains are best known to form homo- or heterodimers or oligomers and to interact with non-SAM protein domains and even RNAs (Qiao and Bowie, 2005). The observation that three SAM domains in tandem are required for binding to a target protein is unprecedented. The structure of the liprin- $\alpha 2$ _LH/CASK_CaMK complex also explains why the extended SAM1 (corresponding to the canonical SAM1 and the insertion between SAM1 and SAM2) is not sufficient for liprin- $\alpha 2$ to bind to CASK (Figures 1C and 1D).

The SAM Repeats of Liprins Form Structural and Functional Supramodules

All liprins contain three highly conserved SAM domains arranged in tandem at their C-terminal ends (Figure 2A). Although sequence similarities are low, the overall folds of the three SAM domains are similar (Figure S1A). In the liprin- $\alpha 2$ structure, the head-to-tail interactions between the three SAM domains lead to the formation of two interdomain interfaces (SAM1/2 and SAM2/3) (Figures 1E and 3A). The head face of SAM1 and the tail side of SAM3 are open in the complex (Figures 1E); as we show below, these open sides mediate the formation of liprin- α/β heterodimers. The SAM domains in liprin- $\alpha 2$ are held

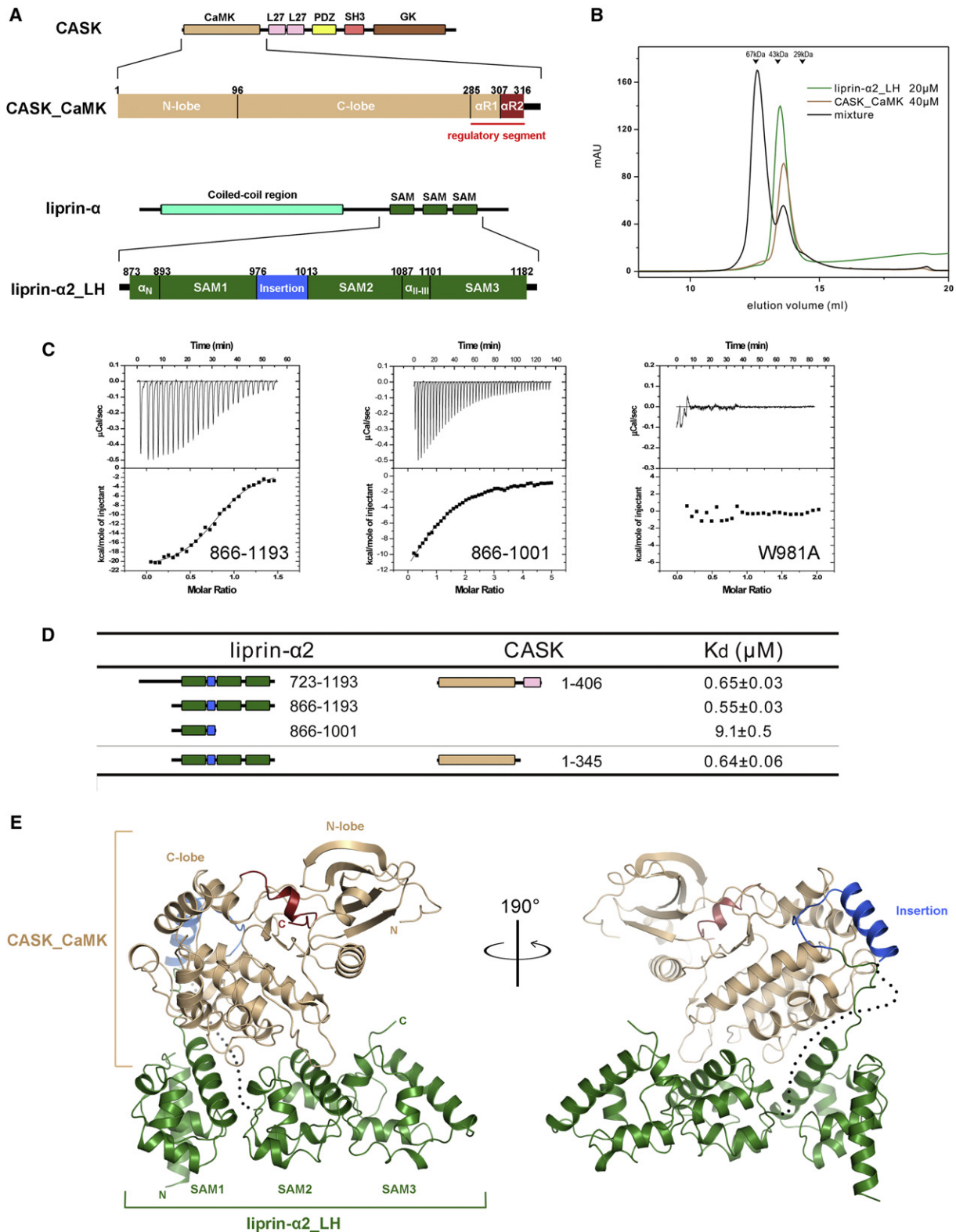


Figure 1. Characterization and the Overall Structure of the Liprin- α 2 and CASK Complex

(A) Schematic diagrams of the domain organizations of liprin- α and CASK. The figure also illustrates the detailed boundaries of the CASK CaMK domain (CASK_CaMK) as well as the three SAM repeats of liprin- α 2 (liprin- α 2_LH). The regulatory segment of CASK_CaMK is underlined. The color coding of the domains is used throughout the entire manuscript except as otherwise indicated.

Table 1. Statistics of Data Collection and Model Refinement

Data Collection		
	Liprin- α 2_LH/ CASK_CaMK	Liprin- α 2_LH/ liprin- β 1_LH
Space group	$P4_12_12$	$P6_1$
Unit cell parameters (Å)	a = b = 78.6, c = 227.4	a = b = 141.9, c = 181.1
Resolution range (Å)	50–2.2 (2.24–2.2)	50–2.9 (2.95–2.9)
No. of unique reflections	36535 (1780)	45715 (2260)
Redundancy	5.9 (4.1)	5.8 (5.2)
I/ σ	20.4 (2.3)	20.5 (2.2)
Completeness (%)	98.6 (96.6)	99.5 (99.5)
R_{merge} (%) ^a	7.8 (55.4)	6.8 (62.3)
Structure Refinement		
Resolution (Å)	50–2.2 (2.26–2.2)	50–2.9 (2.975–2.9)
$R_{\text{cryst}}/R_{\text{free}}$ (%) ^b	19.5 (24.3)/ 23.6 (31.5)	21.4 (27.1)/ 25.8 (39.1)
Rmsd bonds (Å)/angles (°)	0.011/1.2	0.009/1.3
Average B factor	53.5	102.4
No. of atoms		
Protein atoms	4939	8120
Water molecules	110	13
Other molecules	36	30
No. of reflections		
Working set	34,619	42,766
Test set	1818	2263
Ramachandran plot		
Most favored regions (%)	93.2	89.0
Additionally allowed (%)	6.6	11.0
Generously allowed (%)	0.2	0.0

Numbers in parentheses represent the value for the highest-resolution shell.

^a $R_{\text{merge}} = \sum |I_i - I_m| / \sum I_i$, where I_i is the intensity of the measured reflection and I_m is the mean intensity of all symmetry-related reflections.

^b $R_{\text{cryst}} = \sum ||F_{\text{obs}}| - |F_{\text{calc}}|| / \sum |F_{\text{obs}}|$, where F_{obs} and F_{calc} are observed and calculated structure factors. $R_{\text{free}} = \sum_T ||F_{\text{obs}}| - |F_{\text{calc}}|| / \sum_T |F_{\text{obs}}|$, where T is a test data set of about 5% of the total reflections randomly chosen and set aside prior to refinement.

together by H-bonding, hydrophobic, and charge-charge interactions. The interaction between SAM2 and SAM3 is further stabilized by a connecting α helix ($\alpha_{\text{I-III}}$), which physically staples the two domains together (Figure 2B). Consistent with the extensive interdomain interactions observed between SAM2 and 3, we were not able to obtain isolated SAM2 or SAM3 despite numerous trials with different domain boundaries and expres-

sion conditions. SAM1 contains an additional α helix (α_{N}) at its N terminus; the extensive hydrophobic contact between α_{N} and the canonical SAM1 explains why α_{N} is essential for the preparation of stably folded SAM1 and SAM123 (Figure 2C). The interaction between SAM1 and SAM23 is strong, as we were able to obtain a highly stable SAM1/SAM23 complex simply by mixing isolated SAM1 with SAM23 (data not shown). The residues forming the inter-SAM interface in liprins are highly conserved (Figure 2A), suggesting that the linear head-to-tail assembly of the three SAM repeats is a feature common to all liprin isoforms. Since both SAM1 and SAM2 of liprin- α 2 make direct contact with CASK_CaMK in the complex structure (Figures 1D and 1E), the formation of the structurally integrated SAM123 repeats is functionally required for the formation of the liprin- α 2/CASK complex. Taken together, our structural and biochemical analysis reveals that liprin- α 2 SAM123 acts as a structural and functional supramodule with its interaction mode that has not been previously described in SAM domains. Analysis of SAM domain proteins in mammalian genomes shows that a number of proteins contain multiple SAM domain repeats linked closely with each other in their primary sequences (Figure S1B). It is possible that the formation of SAM domain supramodules is a feature shared by many multi-SAM domain proteins. Indeed, a recent structural study of a tandem SAM domain protein called AIDA-1 showed that its two SAM domains indeed form a structural supramodule via a similar head-to-tail interaction mode (Kurabi et al., 2009) (Figure 3A).

Although many head-to-head and tail-to-tail SAM domain interactions have been reported, all known heterotypic SAM dimers or specific SAM oligomers are formed via the head-to-tail assembly mode (Qiao and Bowie, 2005) (Figure 3A), indicating that the head-to-tail SAM domain interaction mode is a conserved property. Unlike SAM oligomers from polyhomeotic (Ph), Sexcomb-on-midleg, TEL, and diacylglycerol kinase δ 1, which form left-handed helical polymers (Harada et al., 2008; Kim et al., 2001, 2002), the three SAM domains in liprin- α 2 are arranged in a linear manner (Figure 3B). The structural differences between the liprin- α 2 SAM repeats and the previously characterized SAM oligomers show that subtle differences in the head-to-tail interactions between two SAM domains can lead to profound differences in the higher-order organizations of SAM oligomers.

The Interaction between CASK and Liprin- α Is Specific to Mammals

Two distinct interfaces involving a total of ~ 3400 Å² surface area mediate the formation of the CASK_CaMK and liprin- α 2. Interface I, which buries ~ 2000 Å² surface area, is formed by SAM1 and 2 of liprin- α 2 and the bottom of the CASK_CaMK

(B) Analytical gel filtration chromatography showing that liprin- α 2_LH and CASK_CaMK form a 1:1 stoichiometric complex. One can note that about half of CASK_CaMK remains in its free form in the elution profile of the CASK_CaMK/liprin- α 2_LH mixture prepared at a 2:1 molar ratio. The elution volumes of the molecular mass markers are indicated at the top.

(C) Example ITC curves showing the mapping of interaction between CASK and liprin- α 2. The left panel shows the binding curve of liprin- α 2_LH(866-1193) with the CASK_CaMK(1-345), the middle panel presents the interaction of the extended SAM1(866-1001) with CASK_CaMK(1-345), and the right panel represents the reaction of liprin- α 2_LH(866-1193) with the W981A mutant of CASK_CaMK(1-345).

(D) The dissociation constants of the binding reactions of various forms of CASK and liprin- α 2 derived from the ITC-based assays.

(E) The overall structure of the liprin- α 2_LH/CASK_CaMK complex with the color coding shown in (A). A 20-residue segment in the SAM1 and 2 insertion with no traceable electron densities is indicated by a dotted line.

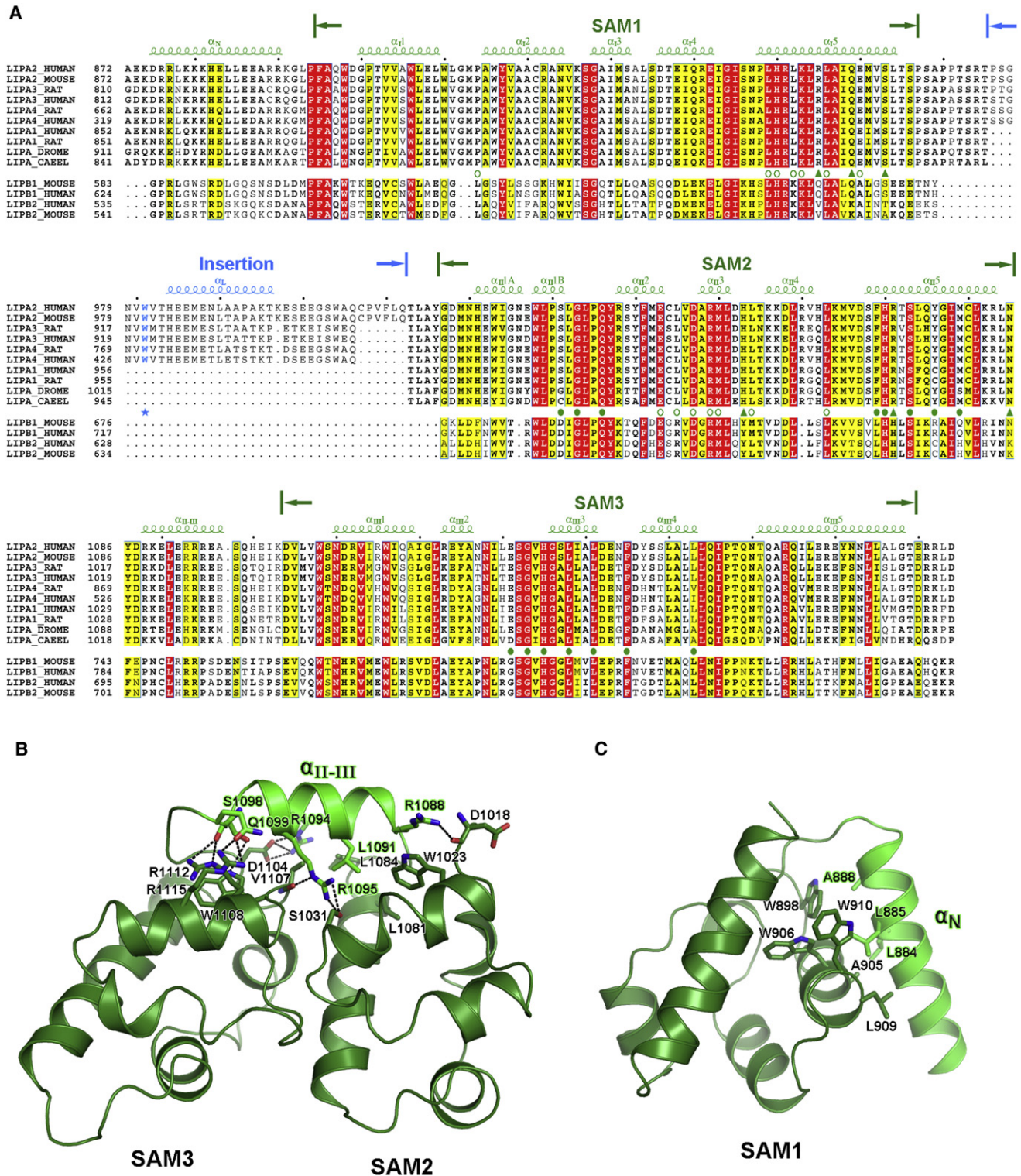


Figure 2. The Supramodular Assembly Mode of the SAM Repeats in Liprins
 (A) The amino acid sequence alignment of the four isoforms of mammalian liprin- α ($\alpha 1$, $\alpha 2$, $\alpha 3$, and $\alpha 4$, indicated by LIPA1, LIPA2, LIPA3, and LIPA4, respectively) and liprin- α from *Drosophila* (LIPA_DROME) and *C. elegans* (LIPA_CAEL), as well as the mammalian liprin- β isoforms ($\beta 1$ and $\beta 2$, shown as LIPB1 and LIPB2, respectively). Residues that are absolutely and highly conserved are shown in red and yellow boxes. The secondary structural elements are labeled above the alignment. The boundaries of the three SAM domains and the insertion between SAM1 and 2 are indicated above the secondary structures following

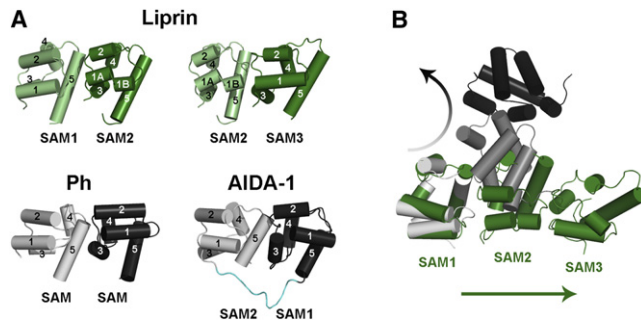


Figure 3. The Unique Assembly Mode of the SAM Repeats in Liprin- α
 (A) Comparisons of the head-to-tail SAM/SAM interactions in liprin- α , in the polyhomeotic-SAM polymer (Ph-SAM, PDB code: 1KW4), and in the SAM tandem of AIDA-1 (PDB code: 2KIV).
 (B) The liprin- α SAM repeats are arranged in a near-linear mode, in contrast to the helical assembly mode of the SAM polymer from Ph-SAM.

C-lobe, and interface II, which buries $\sim 1400 \text{ \AA}^2$ surface area, is formed by a ~ 25 -residue insertion connecting SAM1 and 2 of liprin- $\alpha 2$ with one side of CaMK C-lobe (Figure 1C). Interface I contains three salt bridges (Arg955_{SAM1}-Glu263_{CaMK}, His1053_{SAM2}-Glu269_{CaMK}, and Arg1071_{SAM2}-Glu171_{CaMK}) and several H-bonds (Figure 4A), explaining why SAM2 is required for liprin- $\alpha 2$ to bind to CaMK. We measured the impact of several point mutations of liprin- $\alpha 2$ and CaMK_CaMK that disrupted the salt bridges (R995E_{SAM1}, H1053E_{SAM2}, and E269A_{CaMK}) on complex formation. The disruption of each bridge led to ~ 5 - to 15-fold decreases in the binding affinity of the complex (Figures 4C and S2).

The residues from liprin- $\alpha 2$ that form interface II of the complex are conserved but are strictly limited to the $\alpha 2$, $\alpha 3$, and $\alpha 4$ isoforms of mammalian liprins. This insertion sequence does not exist in liprin- α from *C. elegans* and *Drosophila* and in mammalian liprin- $\alpha 1$ (Figure 2). In the liprin- $\alpha 2$ /CaMK complex, Trp981 from the SAM1 and 2 insertion, together with part of Val980, inserts into a hydrophobic pocket formed by Ile103, Tyr113, Val117, and Tyr121 of CaMK_CaMK (Figure 4B). The Arg106-Phe111 cation- π pair of CaMK, together with two H-bonds formed between Asn154_{CaMK} and the backbone of Trp981, further locks the entire Trp981 into the CaMK hydrophobic pocket (Figure 4B). We predicted that Trp981 should play a critical role in the interaction between liprin- $\alpha 2$ and CaMK. Notably, Trp981 is strictly conserved in all liprin- α isoforms containing the SAM1 and 2 insertion (Figure 2A). In full support of our prediction, the Trp981Ala substitution completely abolished the binding of liprin- $\alpha 2$ to CaMK (Figure 1C, right panel). As expected, the removal of the SAM1 and 2 insertion (aa 976–1012) also completely disrupted liprin/CaMK complex formation (Figures 4C and S2). Since the α helix in the SAM1 and 2 insertion does not make direct contact with CaMK_CaMK, we hypothe-

sized that a short stretch of amino acids centered on Trp981 of liprin- $\alpha 2$ is most critical for binding to CaMK. Indeed, an 8-residue synthetic peptide corresponding to residues 978–985 of liprin- $\alpha 2$ (“GNVWVTHE”) displayed respectable binding to CaMK_CaMK ($K_d \sim 36 \mu\text{M}$) (Figures 4C and S2). It is noted that the SAM1 and 2 insertion of human liprin- $\alpha 2$ is encoded by two short exons (Zürner and Schoch, 2009), suggesting a possible mechanism for the gain of the insertion during evolution.

The SAM1 and 2 Insertion in Liprin- $\alpha 2$ Is Essential for Recruiting CaMK to Presynaptic Boutons

We next examined whether the SAM1 and 2 insertion in liprin- α proteins is important for the assembly of the liprin- α /CaMK complex in neurons. Using coimmunoprecipitation (coIP) experiments, we found that the full-length liprin- $\alpha 2$ binds significantly more CaMK than liprin- $\alpha 1$. As a control, both liprin- α s bind to RIM1 with equal efficiency, as they share the same RIM1 binding sequence in their N-terminal coiled-coil regions (Figure 5C). CoIP experiments using a liprin- $\alpha 1$ chimera that contains the liprin- $\alpha 2$ SAM1 and 2 insertion (“GFP-liprin- $\alpha 1$ (Ins)”) (Figure 5B), showed increased CaMK binding compared to GFP-liprin- $\alpha 1$ (Figure 5C), confirming the pivotal role of the SAM1 and 2 insertion in liprin- $\alpha 2$ for binding to CaMK.

We next tested whether the SAM1 and 2 insertion is important for the presynaptic localization of endogenous CaMK in cultured hippocampal neurons. Interestingly, a marked increase in presynaptic CaMK was observed in neurons overexpressing liprin- $\alpha 2$ ($\sim 48\%$) compared to neurons expressing GFP-liprin- $\alpha 1$ and GFP alone (Figures 5D and 5E). Expression of GFP-liprin- $\alpha 1$ (Ins) in hippocampal neurons increased synaptic CaMK staining by 23% compared to GFP-liprin- $\alpha 1$ (Figures 5D and 5E). As expected, the synaptic RIM intensities were not significantly different in neurons expressing the three forms of the liprin (Figure 5F). These experiments show that the interaction of the full-length liprin- $\alpha 2$ with CaMK is dependent on the SAM1 and 2 insertion and that this region is important for recruiting CaMK to mature hippocampal presynapses.

The above structural, biochemical, and cellular analyses clearly demonstrate that the SAM1 and 2 insertion is strictly required for liprin- $\alpha 2$ (and $\alpha 3$ and $\alpha 4$, as well) to bind to CaMK. More importantly, the above data reveal that liprin- $\alpha 1$ in mammals and liprin- α from *C. elegans* and *Drosophila* do not bind to CaMK/Lin-2, providing a clear mechanistic explanation for findings from the genetic and biochemical studies showing that liprin- α and CaMK/Lin-2 do not interact with each other in *C. elegans* and *Drosophila*. Since liprins can form oligomers through both homo- and heterodimerization (Serra-Pagès et al., 1998; see below for more details), mammalian liprin- α is capable of linking the Veli/CaMK/Mint-1 master scaffold to the liprin- α -assembled presynaptic protein complexes shared by all eukaryotes (e.g., LAR, ELKS, RIM, and GIT1) (Ko et al., 2003a, 2003b; Serra-Pagès et al., 1998). The addition of the

the color scheme shown in Figure 1A. The residues in SAM domains that form extensive contacts with CaMK-CaMK are labeled with triangles. Trp981 in the SAM1 and 2 insertion, which plays a paramount role for liprin- $\alpha 2$ to bind to CaMK, is highlighted with a star and colored in blue. The residues that are important for inter-SAM domain interactions are also indicated (open circles for the inter-SAM1/2 interface and filled circles for the inter-SAM2/3 interface).

(B) The connecting α helix, α_{I-III} , staples SAM2 and SAM3 together to form an inseparable structural unit.

(C) An additional α helix (α_N) N-terminal to SAM1 stabilizes the domain by extensive hydrophobic contacts.

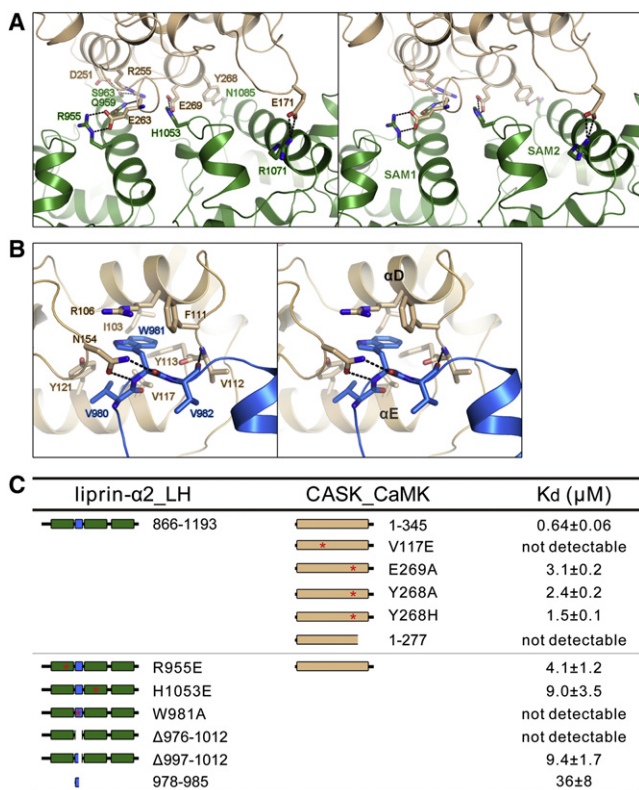


Figure 4. Molecular Details of the Interfaces of the Liprin- α 2_LH/CaMK Complex

(A and B) Detailed interactions showing the interface I (A) of the liprin- α 2_LH/CaMK complex formed by SAM1 and SAM2 of liprin- α 2 with the bottom face of the CaMK C-lobe and the interface II (B) formed by the unique SAM1 and 2 insertion of liprin- α 2 and side of the CaMK C-lobe. In the drawings, the residues involved in the liprin- α 2/CaMK interaction are drawn in the explicit stick model. Hydrogen bonds and salt bridges are indicated by dashed lines.

(C) The impact of the mutations in the two interfaces on the liprin- α 2_LH/CaMK complex formation assessed by measuring the quantitative dissociation constants of the binding reactions using ITC.

Veli/CaMK/Mint-1 master scaffold and its associated proteins to the active zone transmitter release machinery organized by liprin- α provides a possible molecular basis for the more elaborate regulation of synaptic activity in higher eukaryotes.

Specificity Determinants of the CaMK/Liprin- α 2 Interaction

CaM-dependent kinases (e.g., CaMKI, CaMKII, CaMKIV, and DAPKs) share similar kinase domain structures with that of CaMK. However, these CaMKs are not likely to bind to liprin- α , as the critical residues in CaMK that form interfaces I (e.g., Glu171, Glu263, and Glu269) and II with liprin- α are not conserved in other CaMKs (Figure S3A). Moreover, the residue corresponding to Val117 (at the base of the Trp981_{liprin- α 2}-accommodating hydrophobic pocket) in CaMK is instead always a negatively charged Asp or Glu in other CaMKs (Figure S3A). This negatively charged residue and a highly conserved positively charged residue (corresponding

to Arg106 in CaMK) (Figure S3A) in each of these CaMKs form a structurally conserved salt bridge (Figure S3B), which would prevent Trp981_{liprin- α 2} from entering the α D/ α E pocket, as seen in the liprin- α 2/CaMK complex. In our ITC-based analysis, the Val117 to Glu substitution of CaMK indeed completely disrupted its binding to liprin- α 2 (Figures 4C and S2), presumably because of the formation of a salt bridge between Arg106 and Glu117. Collectively, the above structural and biochemical analyses provide a mechanistic explanation for the high specificity of liprin- α 2 for CaMK. Finally, the Val117Glu-CaMK may be useful as a specific binding-defective mutant for studying the functions of the liprin- α /CaMK complex in vivo.

CaMK Adopts an Open Conformation in the Liprin- α 2/CaMK Complex

The overall structure of CaMK in the liprin- α 2/CaMK complex is highly similar to the structure of the isolated CaMK bound to nucleotides (referred to as CaMK_{nuc}) (Mukherjee et al., 2008). In particular the conformations of the N- and C-lobes of CaMK in the two structures are essentially identical (rmsd of \sim 0.8 Å for N-lobe and \sim 0.6 Å for C-lobe). However, the structures of CaMK in the liprin- α 2/CaMK complex and in CaMK_{nuc} do differ in several important aspects. First, both α R1 and α R2, the two regulatory α helices at the C-terminal end of the C-lobe in all CaM-dependent kinases, are clearly defined in the CaMK structure of the liprin- α 2/CaMK complex (Figure S3A). Importantly, α R2, which is disordered in CaMK_{nuc}, inserts into the nucleotide-binding cleft, thereby preventing ATP from binding to the CaMK domain in the liprin- α 2/CaMK complex (Figure S4A). The corresponding α R2 segments in other CaM-dependent kinases (e.g., CaMKI and twitchin kinase) in their autoinhibited forms are also found to insert into their respective catalytic clefts (Goldberg et al., 1996; Hu et al., 1994). Second, the relative orientations of the N- and C-lobes in the two CaMK structures are different. The N-lobe of CaMK in the liprin- α 2/CaMK complex is rotated by \sim 12° anticlockwise compared to the CaMK_{nuc} structure, and this difference in orientation between the two lobes may be the result of the insertion of α R2 into the nucleotide binding pocket (Figure S4A). Therefore, the CaMK domain of CaMK in the liprin- α 2/CaMK complex adopts an open and inactive conformation.

The regulatory sequences of CaMK and that of CaMKII α are essentially identical (Figure S4B), suggesting that CaMK binds to CaM in a Ca²⁺-dependent manner. Indeed, analytical gel filtration-based assays showed that CaM binds to CaMK with a high affinity in a Ca²⁺-dependent manner (Figure S4C), confirming that the regulatory sequence of CaMK contains a CaM binding motif. We further showed that the binding of Ca²⁺-CaM has no impact on CaMK/liprin- α 2 complex formation (Figure S4C).

XLMR Mutations of CaMK

The central role that CaMK plays in the development of mammals is demonstrated by the lethal phenotype of CaMK null mutants (Atasoy et al., 2007; Najm et al., 2008). Mild mutations (e.g., point substitutions, truncations of internal fragments, or decreased

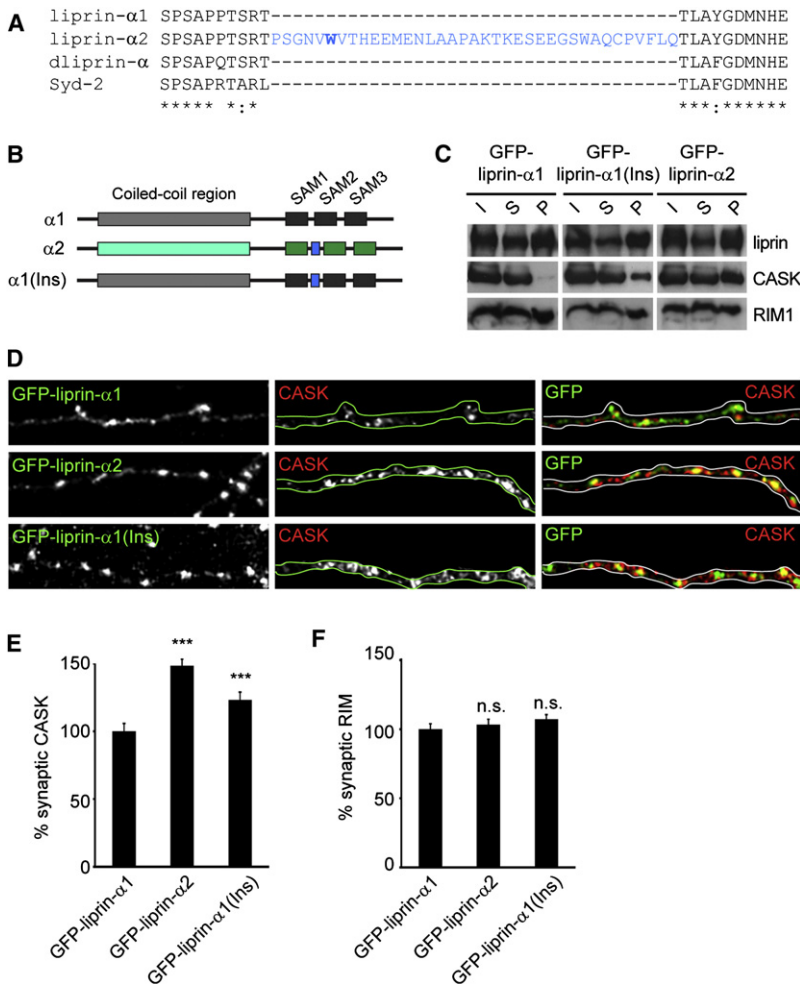


Figure 5. Liprin- α 2/CASK Interaction Induces Presynaptic Targeting of CASK in Hippocampal Neurons

(A) Alignment of the region between the first and second SAM domains of human liprin- α 1, α 2, *Drosophila* dliprin- α , and *C. elegans* Syd-2. The 37-residue linker is indicated in blue.

(B) Schematic diagram of the liprin- α 1, α 2, and mutant α 1(Ins) expression constructs. A small box in blue indicates the presence of a 37-residue linker region between the first and second SAM domains.

(C) Western blots of immunoprecipitation of GFP-liprin- α 1/ α 2/ α 1(Ins) and colIP of HA-CASK or RIM1 (untagged) from HEK293 cell extracts.

(D) Representative images of hippocampal neurons transfected with GFP-liprin- α 1/ α 2/ α 1(Ins) expression constructs and imaged for GFP (green) and endogenous CASK (red).

(E) Quantification of fluorescence intensity of endogenous CASK at presynaptic sites transfected with GFP-liprin- α expression constructs (GFP-liprin- α 1: 100.0% ± 5.8%, GFP-liprin- α 2: 148.3% ± 4.8%, GFP-liprin- α 1(Ins): 123.2% ± 5.8%; n = 100 synapses per group; ***, t test, p < 0.0005). Intensity of synaptic CASK labeling in GFP-liprin- α 1-expressing neurons was set to 100%. The error bars represent the standard error of the mean (SEM) of the total number of synapses analyzed.

(F) Quantification of fluorescence intensity of endogenous RIM at presynaptic sites transfected with GFP-liprin- α expression constructs (GFP-liprin- α 1: 100.0% ± 3.9%, GFP-liprin- α 2: 103.2% ± 4.0%, GFP-liprin- α 1(Ins): 107.2% ± 3.3%; n = 100 synapses per group). Intensity of synaptic RIM labeling in GFP-liprin- α 1-expressing neurons was set to 100%. The error bars represent SEM of the total number of synapses analyzed.

expression levels), three of which occur in the CASK_CaMK region (Najm et al., 2008; Piluso et al., 2009; Tarpey et al., 2009), have recently been reported to cause XLMR in humans (Froyen et al., 2007; Hayashi et al., 2008; Najm et al., 2008; Piluso et al., 2009; Tarpey et al., 2009). These mutations have diverse effects on CASK expression and the CASK/liprin- α 2 interaction. The 83G → T CASK mutation is a missense mutation that leads to the substitution of Arg28 in the N-lobe of CaMK with Leu. This missense mutation may not directly affect CASK-CaMK function; instead, it has been shown to cause the partial skipping of exon2 of CASK (Piluso et al., 2009), leading to lower amounts of the protein. The dosage dependence of CASK in the involvement of XLMR has also been demonstrated in another study, which showed that haploinsufficiency of CASK may cause the disease (Froyen et al., 2007). These human genetic studies indicate that even subtle protein level alterations can drastically alter neuronal circuit function, possibly by shifting the equilibriums of CASK with its myriad binding partners.

In addition to XLMR mutations that affect CASK protein levels, there are mutations that are associated with XLMR that disrupt CASK/liprin- α 2 binding. The 802T → G CASK mutation that causes XLMR is a missense mutation leading to the substitution

of Tyr268 with His (Najm et al., 2008; Tarpey et al., 2009). The structure of the liprin- α 2/CASK_CaMK complex reveals that the side chain of Tyr268 forms an H-bond with Asn1058 of liprin- α 2 SAM2 (Figure 4A). The substitution of Tyr268 with His or Ala leads to an ~3- to 4-fold decrease in the affinity of CASK_CaMK for liprin- α 2 (Figure 4C). Given the dosage-dependent activity of CASK in brain functions, mild liprin- α 2 binding affinity changes such as that induced by the Y268H mutation of CASK could contribute to the alteration of cognitive functions observed in XLMR patients. The 915G → A CASK mutation leads to the skipping of exon9, which encodes α K, α R1, and part of the CaM binding domain of CASK_CaMK (aa 278–305) (Figure S3A), and the mutation causes microcephaly (Najm et al., 2008). We investigated the interaction of a truncated CASK_CaMK(1-277) with liprin- α 2; surprisingly, we found that no binding could be detected both in ITC- (Figure 4C) and gel filtration-based assays (Figure 6A). As a control, we demonstrated that CASK_CaMK(1-277) is properly folded (Figure S5) and stable in a urea-induced denaturation assay (data not shown). Since CaM binding to α R2 does not alter the liprin- α 2/CASK_CaMK interaction (Figures S4B and S4C), the loss of liprin- α 2 binding of CASK_CaMK(1-277) is likely the result of conformational changes in CASK_CaMK induced by the truncation of α R1. The structure of the liprin- α 2/CASK_CaMK complex

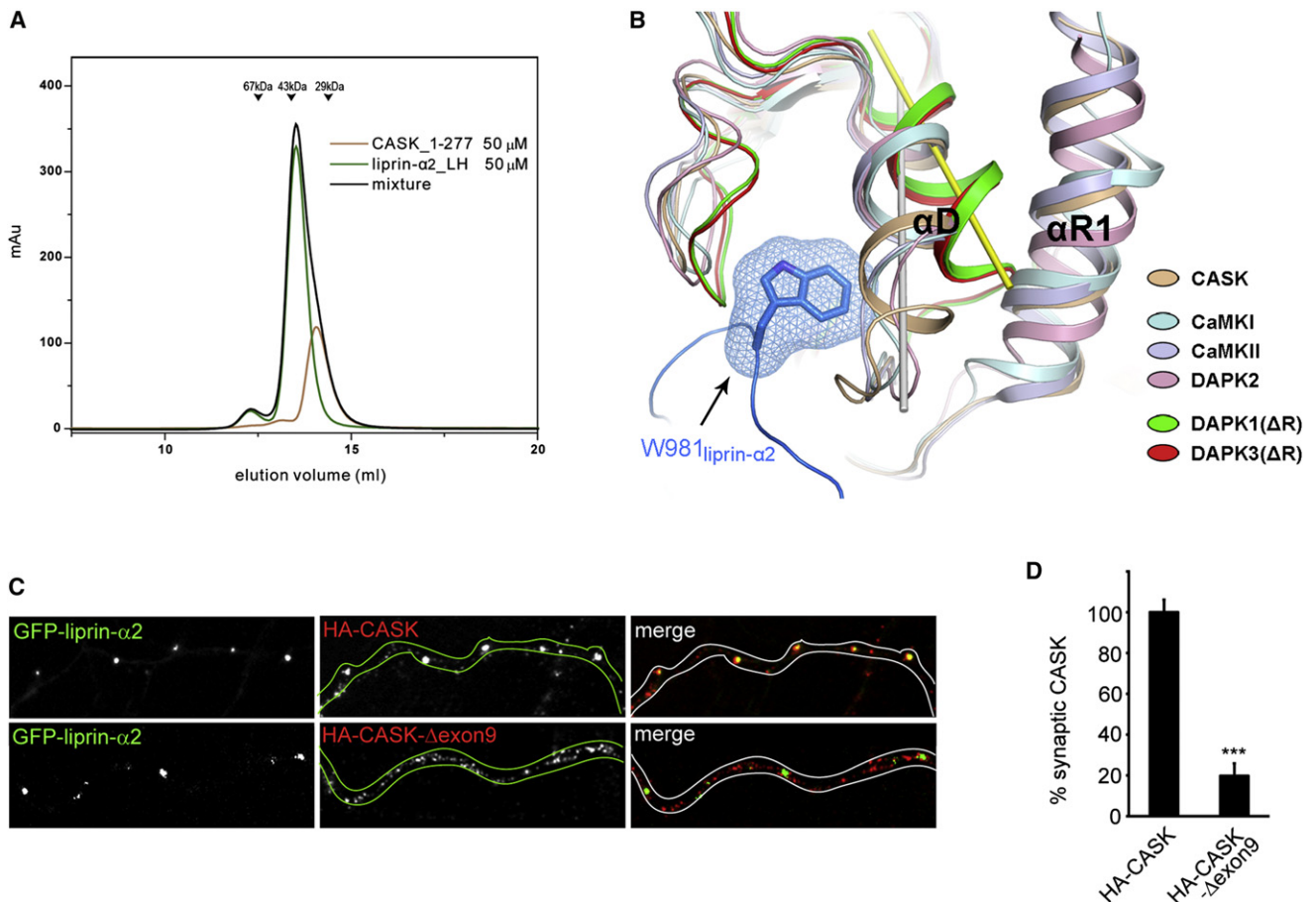


Figure 6. The Exon9 Skipping-Induced Deletion of α R1 Disrupts the Liprin- α 2/CaSK Interaction

(A) Analytical gel filtration profiles of the isolated liprin- α 2_LH, CASK_CaMK(1-277), and a mixture containing equal molar amounts of the two proteins showing no interaction between liprin- α 2 and the truncated CASK_CaMK lacking α R1. The elution volumes of the molecular mass markers are indicated.

(B) Structural comparison of the Trp981_{liprin- α 2}-accommodating hydrophobic pocket of CASK_CaMK with the corresponding regions in other CaM-binding kinases. In this comparison, CaMKI (PDB code: 1A06), CaMKII (2BDW), and DAPK2 (2A2A) contain the full CaMK domains (i.e., the minimal kinase domain plus the regulatory α R1 and α R2 elements), whereas DAPK1 (1JKS) and DAPK3 (3BQR) were crystallized with constructs lacking the regulatory α R1 and α R2 segments. The axes of α D in the full CaMK and the regulatory segment-truncated CaMK structures are indicated by a gray and a yellow rod, respectively. The SAM1 and 2 insertion and the side-chain of Trp981 (highlighted with the meshed surface) of liprin- α 2 are also included in the display.

(C) Representative images of hippocampal neurons cotransfected with GFP-liprin- α 2 and HA-CaSK or HA-CaSK- Δ exon9 expression constructs and imaged for GFP (green) and anti-HA (red).

(D) Quantification of fluorescence intensity of HA-CaSK at presynaptic sites transfected with GFP-liprin- α 2 expression constructs (HA-CaSK: 100.0% \pm 3.7%, HA-CaSK- Δ exon9: 19.8% \pm 6.1%; n = 50 synapses per group; ***, t test, p < 0.0005). Intensity of synaptic HA-CaSK labeling in GFP-liprin- α 2-expressing neurons was set to 100%. The error bars represent SEM of the total number of synapses analyzed.

reveals that the α R1 helix interacts intimately with α D, thus positioning Arg106 in the middle of α D and Phe111 immediately following α D of CASK_CaMK to interact with Trp981 from liprin- α 2 (Figures 4B and 6B). The positions of the α D helix in the structures of CaM-dependent kinases containing α R1 (e.g., CaMKI, CaMKII, and DAPK1/2/3) are similar to that of the α D helix of CASK_CaMK in complex with liprin- α 2. Interestingly, DAPK1 and DAPK3 were also crystallized in the absence of their respective α R1 helices (Figure 6B, green and red ribbons). The removal of α R1 in both DAP kinases led to a \sim 30° outward rotation of α D, presumably due to the removal of the constraints imposed by α R1 (Figure 6B). Similar α D movement is likely to occur in CASK-CaMK when α R1 is removed due to the exon9

skipping. The exon9 skipping-induced α D movement may cause the opening of the Trp981_{liprin- α 2} binding pocket (Figures 4B and 6B), thus disrupting the CASK/liprin- α 2 interaction. Consistently, singly expressed HA-CaSK in hippocampal neurons was found largely diffused in axons (data not shown). Coexpression of liprin- α 2 did not induce the synaptic targeting of a CASK construct that lacks exon9 (HA-CaSK- Δ exon9), as it did to wild-type HA-CaSK (\sim 80% difference) (Figures 6C and 6D). However, it should be pointed out that XLMR caused by CASK mutations could occur via mechanisms unrelated to liprins. Regardless of the exact mechanism underlying CASK mutation-linked XLMR, the structure of CASK_CaMK provides a basis for future functional studies of the involvement of CASK

in the disease. Additionally, the above data suggest that liprin- α 2 interactions play an important role in targeting CASK to presynapses and that the disruption of this interaction may lead to some forms of XLMR.

Structure of the Liprin- $\alpha_{\Delta\text{Insertion}}$ -LH/Liprin- β -LH Heterodimer

To further characterize the role that liprins play in signaling complex organization, we studied the interaction between the α and β isoforms of liprins. As observed in liprin- α , the SAM repeats of liprin- β also adopt a stable monomer in solution (Figure 7A). We demonstrate that α -LH and β -LH form a specific heterodimer when mixed together (Figure 7A). The formation of the α/β -LH heterodimer does not depend on the presence of the SAM1 and 2 insertion, as its deletion from α 2-LH (α 2-LH $_{\Delta\text{Insertion}}$) does not affect the heterodimer formation (Figures 7A and S6). Thus, formation of the α/β -LH heterodimer is a property common to all isoforms of the two liprin subfamilies. An ITC-based binding assay revealed that the LH- α 2 and LH- β 1 complex has a K_d of $\sim 5 \mu\text{M}$ (Figure S6).

We next solved the crystal structure of the α 2-LH $_{\Delta\text{Insertion}}$ / β 1-LH complex at a 2.9 Å resolution (Table 1). Although the resolution of the structure is low and the average B factor of the final refined model is very high, the overall assembly mode and the interactions in the interface between α 2-LH and β 1-LH can be clearly interpreted. Like α 2-LH, β 1-LH contains three SAM domains arranged in a head-to-tail manner (Figure 7B). SAM1 of α 2-LH interacts with SAM3 of β 1-LH via the head-to-tail SAM domain assembly mode, burying a total of $\sim 1000 \text{ \AA}^2$ surface area. The α 2-LH/ β 1-LH complex forms an elongated rod-shaped structure (Figure 7B). Despite their low sequence identity, α 2-LH and β 1-LH have similar overall structures, with an rmsd of 1.8 Å (Figure S7A). A major structural difference between the two SAM repeats is that β 1-LH lacks the α_N helix seen in α -LH SAM1. Instead, β 1-LH contains an additional helix at the C terminus of SAM3 (α_C) (Figures 7B and S7A). This structural difference is likely to play a role in the distinct target binding properties of the two subfamilies of liprins (e.g., α -LH, but not β -LH, can specifically bind to LAR) (Serra-Pagès et al., 1998).

The unbiased simulated annealing omit maps of the residues in the interface of the liprin- α/β complex (Figure S7B) show that the quality of the structure model is reasonably good and the intermolecular interactions are clearly interpretable. The SAM1 $_{\alpha 2}$ /SAM3 $_{\beta 1}$ interaction includes hydrogen bonding, hydrophobic, as well as charge-charge interactions between the residues in α_3 and α_4 of α 2-LH and those in α_{11} and α_5 of β 1-LH (Figures 7C and S7C). Among the residues in the α -LH/ β -LH complex, Arg823 $_{\beta 1}$ and Glu782 $_{\beta 1}$ form salt bridges with Glu938 $_{\alpha 2}$ and Lys926 $_{\alpha 2}$, respectively. Breaking either of these salt bridges through mutagenesis disrupts the interaction between α 2-LH and β 1-LH (Figure S6). Leu820 $_{\beta 1}$, which is strictly conserved in liprin- β and is located at the center of the SAM1 $_{\alpha 2}$ /SAM3 $_{\beta 1}$ interface, inserts into a hydrophobic pocket formed by four highly conserved hydrophobic residues (Val925 $_{\alpha 2}$, Ile930 $_{\alpha 2}$, Leu934 $_{\alpha 2}$, and Ile943 $_{\alpha 2}$) in SAM1 $_{\alpha 2}$ (Figure 7C). Consistent with this analysis, disrupting this hydrophobic interaction totally abolishes α 2-LH/ β 1-LH complex formation (Figure S6). Glu942 $_{\alpha 2}$ contributes to the α 2-LH/ β 1-LH interaction by forming hydrogen bonds

with two main-chain atoms in SAM3 $_{\beta 1}$ and thus fixing the position of Leu820 $_{\beta 1}$ for the interdomain hydrophobic interaction mentioned above. Accordingly, the substitution of Glu942 $_{\alpha 2}$ with Ala eliminates the β 1-LH binding capacity of α 2-LH (Figure S6).

The α 2-LH $_{\Delta\text{Insertion}}$ / β 1-LH structure also provides clear explanations as to why α -LH and β -LH do not form homo-oligomers and why the α 2-LH/ β 1-LH complex exists only as a heterodimer instead of a polymer, even though the potential binding sites of SAM3 $_{\alpha 2}$ and SAM1 $_{\beta 1}$ are open in the heterodimer and neither SAM1 $_{\alpha 2}$ α_N nor SAM3 $_{\beta 1}$ α_C would occlude head-to-tail SAM/SAM interactions (Figure 7B). Specifically, the residue corresponding to Leu820 $_{\beta 1}$ in liprin- α SAM3 is a conserved Gln, explaining why SAM3 of liprin- α cannot interact with SAM1 of liprin- α or β to form liprin- α homo-oligomers or to allow further oligomerization of the α 2-LH/ β 1-LH heterodimer (Figures 7C and S7C). Although the residues in SAM1 $_{\alpha 2}$ forming the SAM3 $_{\beta 1}$ binding hydrophobic pocket are largely conserved in SAM1 of liprin- β (Figure S7C), the corresponding hydrophobic pocket in SAM3 $_{\beta 1}$ is occluded by a bulky Trp (Trp630 $_{\beta 1}$) at its center, preventing its own SAM1 from binding; this explains why β -LH cannot form head-to-tail homo-oligomers (Figures S6B and S7D). We note with interest that SAM1 is the most conserved SAM domain in α -LH and that SAM3 is the most conserved SAM domain in β -LH throughout evolution (Figure 7B). It is tempting to speculate that, during evolution, the conserved SAM1 $_{\alpha}$ /SAM3 $_{\beta}$ interaction may have limited amino acid sequence diversification of these two SAM domains.

The α -LH/ β -LH Heterodimer Is Open to Organize Supramolecular Protein Complexes

In the α 2-LH $_{\Delta\text{Insertion}}$ / β 1-LH structure, the three SAM domains of α 2-LH adopt essentially the same conformation as those in the liprin- α 2_LH/CASK_CaMK complex (rmsd of 0.7 Å). Importantly, despite being involved in binding to both CASK and β 1-LH, SAM1 $_{\alpha 2}$ uses two completely nonoverlapping surfaces to interact with its two targets (Figures 1E and 7A), suggesting that α 2-LH can bind to CASK and liprin- β simultaneously. Consistent with the above structural analysis, analytical gel filtration chromatography showed that CASK_CaMK, α 2-LH, and β 1-LH interact with each other to form a stable ternary complex in solution (Figure 7D). We built a ternary CASK_CaMK/ α 2-LH/ β 1-LH complex model by superimposing α 2-LH from the CASK_CaMK/ α 2-LH and α 2-LH $_{\Delta\text{Insertion}}$ / β 1-LH complex structures. Consistent with the gel filtration analysis, there is no overlap at all between CASK_CaMK and β 1-LH in the ternary complex model (Figure 7E). Given that liprin- β displays its own unique target binding properties (Serra-Pagès et al., 1998), the liprin- α/β complex can serve as a core scaffold for assembling very large protein complexes involved in the regulation of many cellular functions, including synaptic signaling and development, cell adhesion and migration, and cell polarity (Figure 7F).

In summary, the structures of the liprin- α 2_LH/CASK_CaMK and liprin- α 2_LH $_{\Delta\text{Insertion}}$ /liprin- β 1_LH complexes presented in this work, together with biochemical and cellular studies, reveal that the liprin- α /CASK interaction is a newly acquired function unique to higher eukaryotes and that this interaction may be linked to the higher-order brain functions of mammals. The

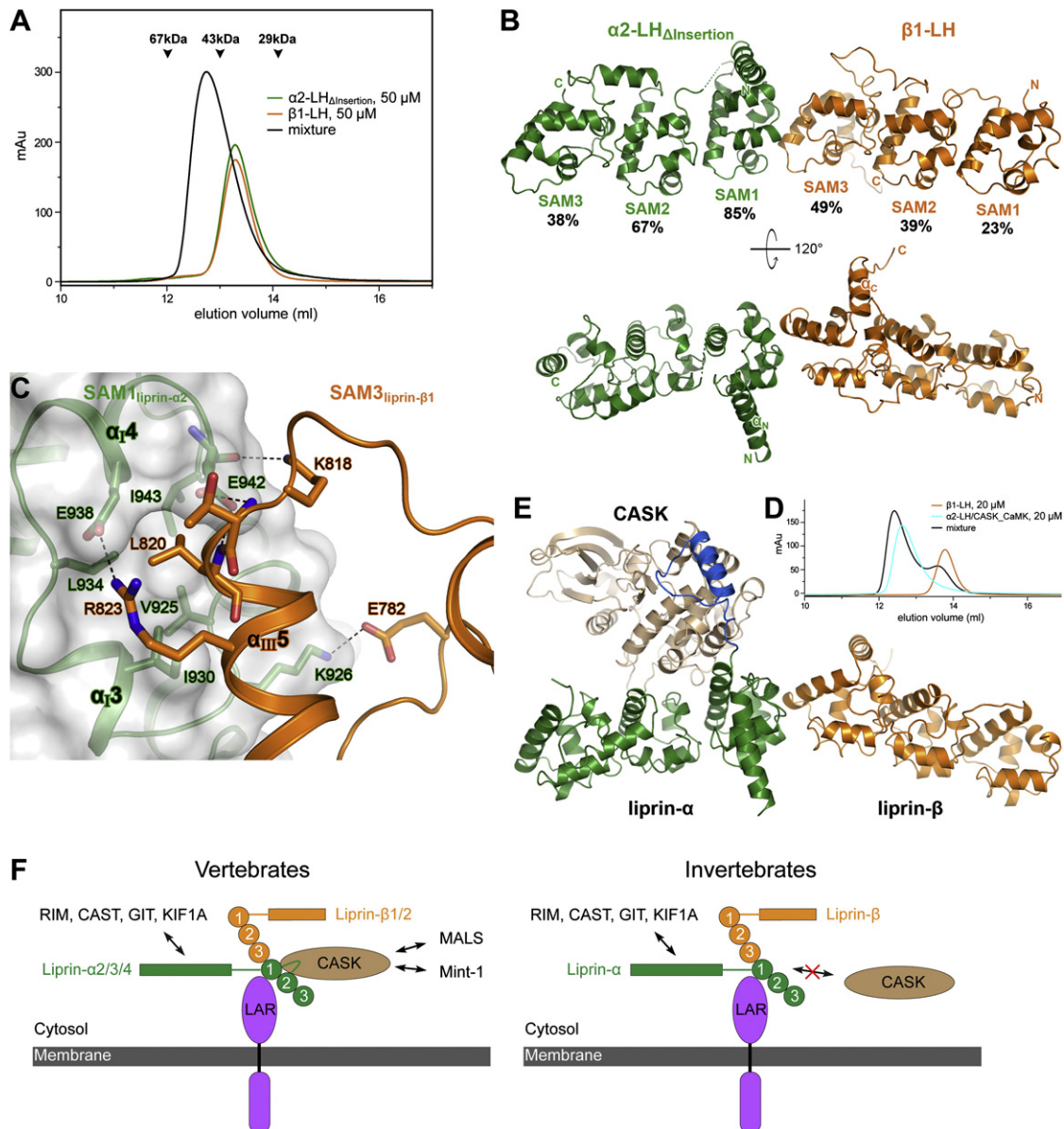


Figure 7. The $\alpha 2$ -LH and $\beta 1$ -LH Form a Head-to-Tail Heterodimer

(A) Analytical gel filtration profiles of $\alpha 2$ -LH $_{\Delta}$ Insertion, $\beta 1$ -LH, and their 1:1 mixture.
 (B) The ribbon representation of the overall structure of the $\alpha 2$ -LH $_{\Delta}$ Insertion/ $\beta 1$ -LH complex. The disordered region in the SAM1/2 loop of $\alpha 2$ -LH is indicated by a dashed line. The percentages of sequence identity of each SAM domain, which are derived from the sequence alignment analysis of members of the liprin- α and liprin- β families found in different species, are indicated below the corresponding domains.
 (C) Molecular details of the $\alpha 2$ -LH/ $\beta 1$ -LH complex interface formed by SAM1 $_{\alpha 2}$ and SAM3 $_{\beta 1}$.
 (D) Analytical gel filtration chromatography showing that the binding of $\beta 1$ -LH to $\alpha 2$ -LH does not interfere with the interaction between CASK_CaMK and $\alpha 2$ -LH.
 (E) The structure model of the CASK_CaMK/ $\alpha 2$ -LH/ $\beta 1$ -LH ternary complex.
 (F) Summary models showing liprin-mediated assembly of large signaling complexes in vertebrates and invertebrates. Binding of LAR to liprin- $\alpha 2$ does not interfere with its interactions with CASK or liprin- β (our unpublished data). The interaction between CASK and liprin- α is specific to vertebrates.

liprin- $\alpha 2$ _LH/CASK_CaMK complex structure also uncovers target binding modes both for the SAM repeats of liprin- α and the kinase-like domain of CASK. The formation of the liprin- α /liprin- β heterodimer provides a molecular basis for the liprin-mediated organization of supramolecular assemblies for diverse

cellular functions. A number of CASK mutations found in XLMR patients have been found to disrupt CASK's binding to liprin- α , and this finding is consistent with the essential roles that liprin- α plays in both brain development and synaptic activity regulation.

EXPERIMENTAL PROCEDURES

Protein Preparation

The LH region (866–1193) of human liprin- α 2 and the LH region (593–853) of mouse liprin- β 1 were expressed in and purified from bacterial cells (see Supplemental Information for detailed construct and protein purification information).

Analytical Gel Filtration Chromatography

Analytical gel filtration chromatography was carried out on an AKTA FPLC system (GE Healthcare) using a Superose 12 10/300 GL column (GE Healthcare) with the column buffer of 50 mM Tris-HCl, 100 mM NaCl, 1 mM DTT (pH 7.5). When necessary, this column buffer was supplemented with either 2 mM CaCl₂ or 1 mM EDTA.

Crystallography

The liprin- α 2_LH/CASK_CaMK complex crystals were obtained by hanging drop vapor diffusion method at 16°C at a complex concentration of 8 mg/ml in the crystallization solution containing 1.4 M (NH₄)₂SO₄, 0.2 M NaCl, 0.1 M MES (pH 6.5). The diffraction data were collected at Shanghai Synchrotron Radiation Facility. The initial phase was determined by molecular replacement using the CASK_CaMK_{nuc} model (PDB code: 3C0G) and the P73 α SAM model (PDB code: 1DXS) as the searching templates. The liprin- α 2_LH $_{\Delta$ Insertion/liprin- β 1_LH complex crystals were also obtained by hanging drop vapor diffusion method at 16°C at a complex concentration of 18 mg/ml in 3%–5% PEG8000, 0.15 M NaCl, 0.1 M Bis-Tris (pH 6.0). The initial phase was determined by molecular replacement using the liprin- α 2_LH structure as the searching model. The detailed X-ray crystallographic methods can be found in the Supplemental Information. All structure figures were prepared by PyMOL (<http://www.pymol.org>).

Isothermal Titration Calorimetry Analysis

All ITC experiments were carried out on a VP-ITC Microcal calorimeter at 25°C. ITC data were analyzed using program Origin7.0 by Microcal (see Supplemental Information for more details).

Cell Culture, Immunocytochemistry, Image Analysis, and Quantification

Details of the constructs for the full-length liprin- α 1, liprin- α 2, CASK, and their derivatives are described in the Supplemental Information. Primary hippocampal cultures, transfections, and immunocytochemistry of cultured neurons are also described in the Supplemental Information.

Confocal images of transfected neurons were acquired on a Zeiss LSM 510 confocal microscope, and images were processed using MetaMorph software (Universal Imaging Corporation). Statistical analysis was performed with Student's *t* test assuming two-tailed distribution and unequal variation (see Supplemental Information for details).

ACCESSION NUMBERS

The atomic coordinates of the liprin- α 2_LH/CASK_CaMK and liprin- α 2_LH $_{\Delta$ Insertion/liprin- β 1_LH complexes have been deposited at the Protein Data Bank under the accession codes of 3TAC and 3TAD, respectively.

SUPPLEMENTAL INFORMATION

Supplemental Information includes Supplemental Experimental Procedures, Supplemental References, and seven figures and can be found with this article online at doi:10.1016/j.molcel.2011.07.021.

ACKNOWLEDGMENTS

We thank the BL17U1 beamline of the Shanghai Synchrotron Radiation Facility for the X-ray beamline time, Zhengguo Wu and Yaru Diao for helping with the kinase activity assays, Lifeng Pan and Jingjing Wu for hydrodynamic analysis of the proteins described in this work, Esther de Graaff for technical assis-

tance, and Anthony Zhang for editing of the manuscript. C.C.H. is supported by Netherlands Organization for Scientific Research (NWO-ALW, NWO-ECHO), Netherlands Organization for Health Research and Development (ZonMw-VIDI, ZonMw-TOP), and a European Science Foundation European Young Investigators (EURYI) Award. M.Z. and Z.W. were supported by grants from the Research Grants Council of Hong Kong to M.Z. (663808, 664009, 660709, 663610, CA07/08.SC01, HKUST6/CRF/10, AoE/B-15/01-II, and SEG_HKUST06) and to Z.W. (662710).

Received: March 14, 2011

Revised: May 3, 2011

Accepted: July 10, 2011

Published: August 18, 2011

REFERENCES

- Astiggarraga, S., Hofmeyer, K., Farajian, R., and Treisman, J.E. (2010). Three Drosophila liprins interact to control synapse formation. *J. Neurosci.* *30*, 15358–15368.
- Atasoy, D., Schoch, S., Ho, A., Nadasy, K.A., Liu, X., Zhang, W., Mukherjee, K., Nosyreva, E.D., Fernandez-Chacon, R., Missler, M., et al. (2007). Deletion of CASK in mice is lethal and impairs synaptic function. *Proc. Natl. Acad. Sci. USA* *104*, 2525–2530.
- Biederer, T., and Südhof, T.C. (2000). Mints as adaptors. Direct binding to neu-rexins and recruitment of munc18. *J. Biol. Chem.* *275*, 39803–39806.
- Borg, J.P., López-Figueroa, M.O., de Taddéo-Borg, M., Kroon, D.E., Turner, R.S., Watson, S.J., and Margolis, B. (1999). Molecular analysis of the X11-mLin-2/CASK complex in brain. *J. Neurosci.* *19*, 1307–1316.
- Choe, K.M., Prakash, S., Bright, A., and Clandinin, T.R. (2006). Liprin-alpha is required for photoreceptor target selection in Drosophila. *Proc. Natl. Acad. Sci. USA* *103*, 11601–11606.
- Dai, Y., Taru, H., Deken, S.L., Grill, B., Ackley, B., Nonet, M.L., and Jin, Y. (2006). SYD-2 Liprin-alpha organizes presynaptic active zone formation through ELKS. *Nat. Neurosci.* *9*, 1479–1487.
- Dunah, A.W., Hueske, E., Wyszynski, M., Hoogenraad, C.C., Jaworski, J., Pak, D.T., Simonetta, K., Liu, G., and Sheng, M. (2005). LAR receptor protein tyrosine phosphatases in the development and maintenance of excitatory synapses. *Nat. Neurosci.* *8*, 458–467.
- Feng, W., Long, J.F., Fan, J.S., Suetake, T., and Zhang, M. (2004). The tetrameric L27 domain complex as an organization platform for supramolecular assemblies. *Nat. Struct. Mol. Biol.* *11*, 475–480.
- Froyen, G., Van Esch, H., Bauters, M., Hollanders, K., Frints, S.G., Vermeesch, J.R., Devriendt, K., Fryns, J.P., and Marynen, P. (2007). Detection of genomic copy number changes in patients with idiopathic mental retardation by high-resolution X-array-CGH: important role for increased gene dosage of XLMR genes. *Hum. Mutat.* *28*, 1034–1042.
- Goldberg, J., Nairn, A.C., and Kuriyan, J. (1996). Structural basis for the auto-inhibition of calcium/calmodulin-dependent protein kinase I. *Cell* *84*, 875–887.
- Harada, B.T., Knight, M.J., Imai, S., Qiao, F., Ramachander, R., Sawaya, M.R., Gingery, M., Sakane, F., and Bowie, J.U. (2008). Regulation of enzyme localization by polymerization: polymer formation by the SAM domain of diacylglycerol kinase delta1. *Structure* *16*, 380–387.
- Hata, Y., Butz, S., and Südhof, T.C. (1996). CASK: a novel dlg/PSD95 homolog with an N-terminal calmodulin-dependent protein kinase domain identified by interaction with neu-rexins. *J. Neurosci.* *16*, 2488–2494.
- Hayashi, S., Mizuno, S., Migita, O., Okuyama, T., Makita, Y., Hata, A., Imoto, I., and Inazawa, J. (2008). The CASK gene harbored in a deletion detected by array-CGH as a potential candidate for a gene causative of X-linked dominant mental retardation. *Am. J. Med. Genet. A.* *146A*, 2145–2151.
- Hofmeyer, K., Maurel-Zaffran, C., Sink, H., and Treisman, J.E. (2006). Liprin-alpha has LAR-independent functions in R7 photoreceptor axon targeting. *Proc. Natl. Acad. Sci. USA* *103*, 11595–11600.
- Hsueh, Y.P., Yang, F.C., Kharazia, V., Naisbitt, S., Cohen, A.R., Weinberg, R.J., and Sheng, M. (1998). Direct interaction of CASK/LIN-2 and syndecan

- heparan sulfate proteoglycan and their overlapping distribution in neuronal synapses. *J. Cell Biol.* 142, 139–151.
- Hu, S.H., Parker, M.W., Lei, J.Y., Wilce, M.C., Benian, G.M., and Kemp, B.E. (1994). Insights into autoregulation from the crystal structure of twitchin kinase. *Nature* 369, 581–584.
- Kaech, S.M., Whitfield, C.W., and Kim, S.K. (1998). The LIN-2/LIN-7/LIN-10 complex mediates basolateral membrane localization of the *C. elegans* EGF receptor LET-23 in vulval epithelial cells. *Cell* 94, 761–771.
- Kaufmann, N., DeProto, J., Ranjan, R., Wan, H., and Van Vactor, D. (2002). *Drosophila* liprin-alpha and the receptor phosphatase Dlar control synapse morphogenesis. *Neuron* 34, 27–38.
- Kim, C.A., Phillips, M.L., Kim, W., Gingery, M., Tran, H.H., Robinson, M.A., Faham, S., and Bowie, J.U. (2001). Polymerization of the SAM domain of TEL in leukemogenesis and transcriptional repression. *EMBO J.* 20, 4173–4182.
- Kim, C.A., Gingery, M., Pilpa, R.M., and Bowie, J.U. (2002). The SAM domain of polyhomeotic forms a helical polymer. *Nat. Struct. Biol.* 9, 453–457.
- Ko, J., Kim, S., Valtschanoff, J.G., Shin, H., Lee, J.R., Sheng, M., Premont, R.T., Weinberg, R.J., and Kim, E. (2003a). Interaction between liprin-alpha and GIT1 is required for AMPA receptor targeting. *J. Neurosci.* 23, 1667–1677.
- Ko, J., Na, M., Kim, S., Lee, J.R., and Kim, E. (2003b). Interaction of the ERC family of RIM-binding proteins with the liprin-alpha family of multidomain proteins. *J. Biol. Chem.* 278, 42377–42385.
- Kurabi, A., Brener, S., Mobli, M., Kwan, J.J., and Donaldson, L.W. (2009). A Nuclear Localization Signal at the SAM-SAM Domain Interface of AIDA-1 Suggests a Requirement for Domain Uncoupling Prior to Nuclear Import. *J. Mol. Biol.* 392, 1168–1177.
- Maximov, A., Südhof, T.C., and Bezprozvanny, I. (1999). Association of neuronal calcium channels with modular adaptor proteins. *J. Biol. Chem.* 274, 24453–24456.
- Mukherjee, K., Sharma, M., Urlaub, H., Bourenkov, G.P., Jahn, R., Südhof, T.C., and Wahl, M.C. (2008). CASK Functions as a Mg²⁺-independent neurexin kinase. *Cell* 133, 328–339.
- Najm, J., Horn, D., Wimplinger, I., Golden, J.A., Chizhikov, V.V., Sudi, J., Christian, S.L., Ullmann, R., Kuechler, A., Haas, C.A., et al. (2008). Mutations of CASK cause an X-linked brain malformation phenotype with microcephaly and hypoplasia of the brainstem and cerebellum. *Nat. Genet.* 40, 1065–1067.
- Olsen, O., Moore, K.A., Fukata, M., Kazuta, T., Trinidad, J.C., Kauer, F.W., Streuli, M., Misawa, H., Burlingame, A.L., Nicoll, R.A., and Brecht, D.S. (2005). Neurotransmitter release regulated by a MALS-liprin-alpha presynaptic complex. *J. Cell Biol.* 170, 1127–1134.
- Olsen, O., Funke, L., Long, J.F., Fukata, M., Kazuta, T., Trinidad, J.C., Moore, K.A., Misawa, H., Welling, P.A., Burlingame, A.L., et al. (2007). Renal defects associated with improper polarization of the CRB and DLG polarity complexes in MALS-3 knockout mice. *J. Cell Biol.* 179, 151–164.
- Patel, M.R., Lehrman, E.K., Poon, V.Y., Crump, J.G., Zhen, M., Bargmann, C.I., and Shen, K. (2006). Hierarchical assembly of presynaptic components in defined *C. elegans* synapses. *Nat. Neurosci.* 9, 1488–1498.
- Piluso, G., D'Amico, F., Saccone, V., Bismuto, E., Rotundo, I.L., Di Domenico, M., Aurino, S., Schwartz, C.E., Neri, G., and Nigro, V. (2009). A missense mutation in CASK causes FG syndrome in an Italian family. *Am. J. Hum. Genet.* 84, 162–177.
- Prakash, S., McLendon, H.M., Dubreuil, C.I., Ghose, A., Hwa, J., Dennehy, K.A., Tomalty, K.M., Clark, K.L., Van Vactor, D., and Clandinin, T.R. (2009). Complex interactions amongst N-cadherin, DLAR, and Liprin-alpha regulate *Drosophila* photoreceptor axon targeting. *Dev. Biol.* 336, 10–19.
- Qiao, F., and Bowie, J.U. (2005). The many faces of SAM. *Sci. STKE* 2005, re7.
- Qiao, F., Harada, B., Song, H., Whitelegge, J., Courey, A.J., and Bowie, J.U. (2006). Mae inhibits Pointed-P2 transcriptional activity by blocking its MAPK docking site. *EMBO J.* 25, 70–79.
- Samuels, B.A., Hsueh, Y.P., Shu, T., Liang, H., Tseng, H.C., Hong, C.J., Su, S.C., Volker, J., Neve, R.L., Yue, D.T., and Tsai, L.H. (2007). Cdk5 promotes synaptogenesis by regulating the subcellular distribution of the MAGUK family member CASK. *Neuron* 56, 823–837.
- Schoch, S., Castillo, P.E., Jo, T., Mukherjee, K., Geppert, M., Wang, Y., Schmitz, F., Malenka, R.C., and Südhof, T.C. (2002). RIM1alpha forms a protein scaffold for regulating neurotransmitter release at the active zone. *Nature* 415, 321–326.
- Seidel, J.J., and Graves, B.J. (2002). An ERK2 docking site in the Pointed domain distinguishes a subset of ETS transcription factors. *Genes Dev.* 16, 127–137.
- Serra-Pagès, C., Medley, Q.G., Tang, M., Hart, A., and Streuli, M. (1998). Liprins, a family of LAR transmembrane protein-tyrosine phosphatase-interacting proteins. *J. Biol. Chem.* 273, 15611–15620.
- Shen, J.C., Unoki, M., Ythier, D., Duperray, A., Varticovski, L., Kumamoto, K., Pedoux, R., and Harris, C.C. (2007). Inhibitor of growth 4 suppresses cell spreading and cell migration by interacting with a novel binding partner, liprin alpha1. *Cancer Res.* 67, 2552–2558.
- Shin, H., Wyszynski, M., Huh, K.H., Valtschanoff, J.G., Lee, J.R., Ko, J., Streuli, M., Weinberg, R.J., Sheng, M., and Kim, E. (2003). Association of the kinesin motor KIF1A with the multimodular protein liprin-alpha. *J. Biol. Chem.* 278, 11393–11401.
- Tarpey, P.S., Smith, R., Pleasance, E., Whibley, A., Edkins, S., Hardy, C., O'Meara, S., Latimer, C., Dicks, E., Menzies, A., et al. (2009). A systematic, large-scale resequencing screen of X-chromosome coding exons in mental retardation. *Nat. Genet.* 41, 535–543.
- Wyszynski, M., Kim, E., Dunah, A.W., Passafaro, M., Valtschanoff, J.G., Serra-Pagès, C., Streuli, M., Weinberg, R.J., and Sheng, M. (2002). Interaction between GRIP and liprin-alpha/SYD2 is required for AMPA receptor targeting. *Neuron* 34, 39–52.
- Zhen, M., and Jin, Y. (1999). The liprin protein SYD-2 regulates the differentiation of presynaptic termini in *C. elegans*. *Nature* 401, 371–375.
- Zürner, M., and Schoch, S. (2009). The mouse and human Liprin-alpha family of scaffolding proteins: genomic organization, expression profiling and regulation by alternative splicing. *Genomics* 93, 243–253.